Supporting Information

For

Revisiting the Oxygen Reduction Reaction Activity of Two-Dimensional TM-C_2N Electrocatalysts via Constant-Potential Density Functional Theory: Crucial Impact of Spin State and Coordination

Yashi Chen[1,2,4], Mingyuan Yu*[1,2,3], Erjun Kan[1,2,3], Si Lan[4], Cheng Zhan*[1,2,3]

[1]Engineering Research Center of Semiconductor Device Optoelectronic Hybrid Integration in Jiangsu Province, Nanjing 210094
[2]MIIT Key Laboratory of Semiconductor Microstructure and Quantum Sensing, Nanjing University of Science and Technology, Nanjing 210094, China
[3]School of Physics, Nanjing University of Science and Technology, Nanjing 210094, China
[4]School of Materials Science and Engineering, Nanjing University of Science and Technology, Nanjing 210094, China

Corresponding author: czhan@njust.edu.cn

Micro-kinetic method:

We assume that the reaction occurs on both the bare TM-C_2N and TM-C_2N with a single coordination. The reaction rate at the site is governed by the rate-limiting step. Thus, the reaction rate can be expressed as:

$$R(U) = \sum k_i(U)[C_i(U)] \#(S1)$$

$$k_i(U) = A_i \exp(\frac{-E_{a,i}}{k_B T}) \exp\left(\frac{-G_i^b(U)}{k_B T}\right) \#(S2)$$

R(U) is the total reaction rate, $C_i(U)$ is the concentration of various possible active sites. A_i, $E_{a,i}$ are effective pre-exponential factor and activation energy, which can be estimated to be 0.26 eV and 1.23×10^9 s^{-1}.[1, 2] k_B is Boltzmann constant. $k_i(U)$ are the reaction rates in corresponding active sites. This can be determined using Eq. S2, derived from classical transition state theory. Additionally, the concentration $G_i^b(U)$ is balanced based on the total site concentration, as given by the following formula:

$$[M] = \sum [C_i(U)] \#(S3)$$

where M is total concentration of active sites, which can be computed by active sites divided by surface area. Besides, $C_i(U)$ follow the equilibrium constants:

$$K_i(U) = \frac{C_i(U)}{C_0(U)} = \exp\left(\frac{-G_i^f(U)}{kT}\right) \#(S4)$$

$C_0(U)$ is concentration of TM-C_2N(IS), the $G_i^b(U)$ is formation energy of various active site relative to TM-C_2N(IS). Finally, the current density can be calculated as:

$$j(U) = \frac{nFR(U)}{N_A} \#(S5)$$

Where n is the charge transfer of reaction, F is Faraday constant, and N_A is the Avogadro constant. It should be noted that there is a limit to the reaction rate of ORR due to the solubility limit of oxygen.[3] The reaction rate changes to:

$$k_i(U) = \exp\left(\frac{-E_{a,i}}{k_B T}\right) min(A_i exp\left(\frac{-G_i^b(U)}{k_B T}\right), v_{O_2}) \#(S6)$$

The values of v_{O_2} is taken as 1×10^8 s^{-1}.[4]

Table S1. Spin state and parameters of free energy fitting for each ORR intermediate.

model	Spin	C (e/V)	U_0 (V/SHE)	E_0 (eV)	E_{ZPE}-T^*S (eV)
TiC_2N*	1	2.39	-2.86	-662.71	0.22
TiC_2N*OOH	1/2	2.87	-2.68	-678.80	0.61
TiC2N*O	0	2.38	-2.71	-670.63	0.29
TiC_2N*OH	1/2	2.32	-2.79	-674.50	0.52
TiC_2NOH*OOH	0	2.45	-2.70	-690.38	0.92
TiC_2NOH*O	0	2.59	-2.48	-683.08	0.58
TiC_2NOH*OH	0	2.48	-2.67	-686.34	0.84
VC_2N*	3/2	2.78	-2.63	-663.18	0.25
VC_2N*OOH	1	2.86	-2.58	-679.60	0.54
VC2N*O	1/2	2.97	-2.51	-671.26	0.30
VC_2N*OH	1	3.05	-2.55	-675.22	0.54
VC_2NOH*OOH	1	2.64	-2.52	-691.68	0.87
VC_2NOH*O	1/2	2.58	-2.49	-683.48	0.60
VC_2NOH*OH	1	2.45	-2.56	-687.11	0.84

CrC_2N*	2	2.32	-2.00	-659.70	0.23
CrC_2N*OOH	3/2	2.19	-1.84	-675.60	0.61
CrC2N*O	1	2.61	-1.65	-666.81	0.28
CrC_2N*OH	3/2	2.19	-1.79	-671.42	0.54
CrC_2NOH*OOH	3/2	2.43	-1.70	-686.82	0.86
CrC_2NOH*O	1	2.70	-1.61	-677.99	0.60
CrC_2NOH*OH	3/2	2.26	-1.73	-682.57	0.83
MnC_2N*	5/2	2.36	-2.08	-659.72	0.20
MnC_2N*OOH	2	2.15	-1.84	-675.97	0.60
MnC2N*O	5/2	2.54	-1.65	-666.51	0.30
MnC_2N*OH	2	2.10	-1.85	-671.77	0.50
MnC_2NOH*OOH	2	2.71	-1.56	-687.07	0.87
MnC_2NOH*O	2	3.02	-1.41	-677.89	0.61
MnC_2NOH*OH	2	2.45	-1.64	-682.60	0.89
FeC_2N*	2	0.92	-0.64	-636.83	0.25
FeC_2N*OOH	3/2	0.73	-0.36	-652.12	0.57
FeC2N*O	2	0.80	0.13	-642.86	0.29
FeC_2N*OH	3/2	1.15	0.24	-648.17	0.53
FeC_2NOH*OOH	2	0.77	0.04	-662.94	0.83
FeC_2NOH*O	3/2	0.95	0.82	-653.39	0.56
FeC_2NOH*OH	2	0.82	0.29	-658.89	0.80
CoC_2N*	3/2	0.95	-0.49	-634.94	0.24
CoC_2N*OOH	1	0.72	-0.24	-650.40	0.54
CoC2N*O	3/2	0.87	0.37	-641.03	0.27
CoC_2N*OH	1	0.77	0.05	-646.20	0.52
CoC_2NOH*OOH	3/2	0.94	0.44	-660.97	0.81
CoC_2NOH*O	3/2	1.04	0.94	-651.47	0.58
CoC_2NOH*OH	3/2	0.92	0.50	-656.76	0.82
NiC_2N*	1	1.40	0.17	-633.61	0.25
NiC_2N*OOH	1/2	0.87	0.25	-648.38	0.55
NiC2N*O	1	0.99	0.73	-638.94	0.26
NiC_2N*OH	1/2	0.81	0.22	-644.47	0.53
NiC_2NOH*OOH	1	0.82	0.65	-658.82	0.84
NiC_2NOH*O	1/2	0.92	0.67	-648.66	0.56
NiC_2NOH*OH	0	1.12	0.85	-653.97	0.81
CuC_2N*	0	0.59	-0.58	-632.07	0.22
CuC_2N*OOH	0	0.89	0.43	-647.02	0.53
CuC2N*O	1/2	0.92	0.68	-637.00	0.23

CuC_2N*OH	0	0.84	0.34	-642.63	0.49
CuC_2NOH*OOH	1/2	0.79	0.46	-657.13	0.80
CuC_2NOH*O	1/2	1.17	1.12	-646.76	0.47
CuC_2NOH*OH	1/2	1.17	1.10	-652.74	0.77

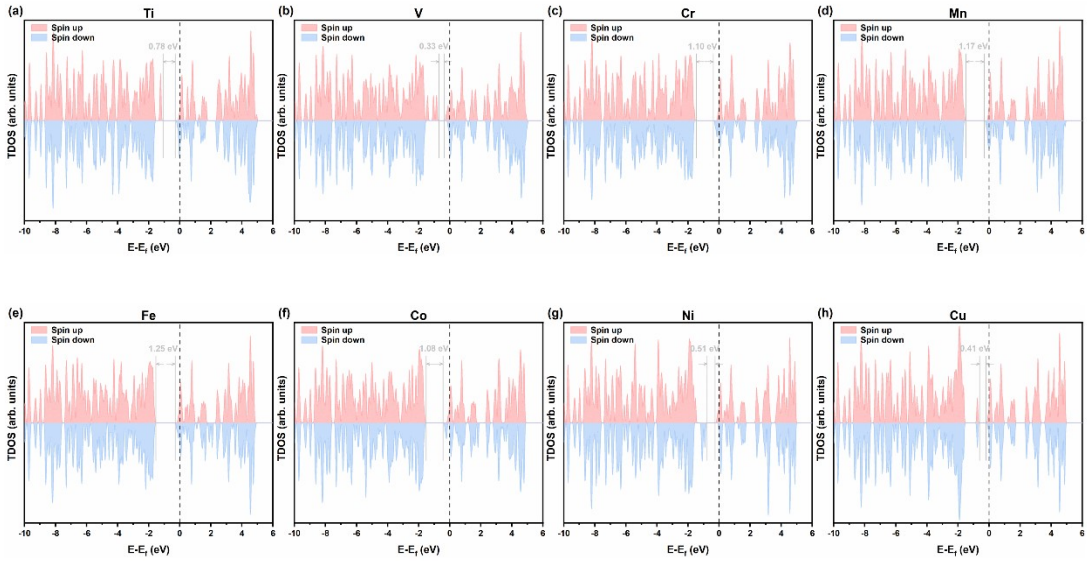

Figure S1. The total density of states of TM-C_2N.

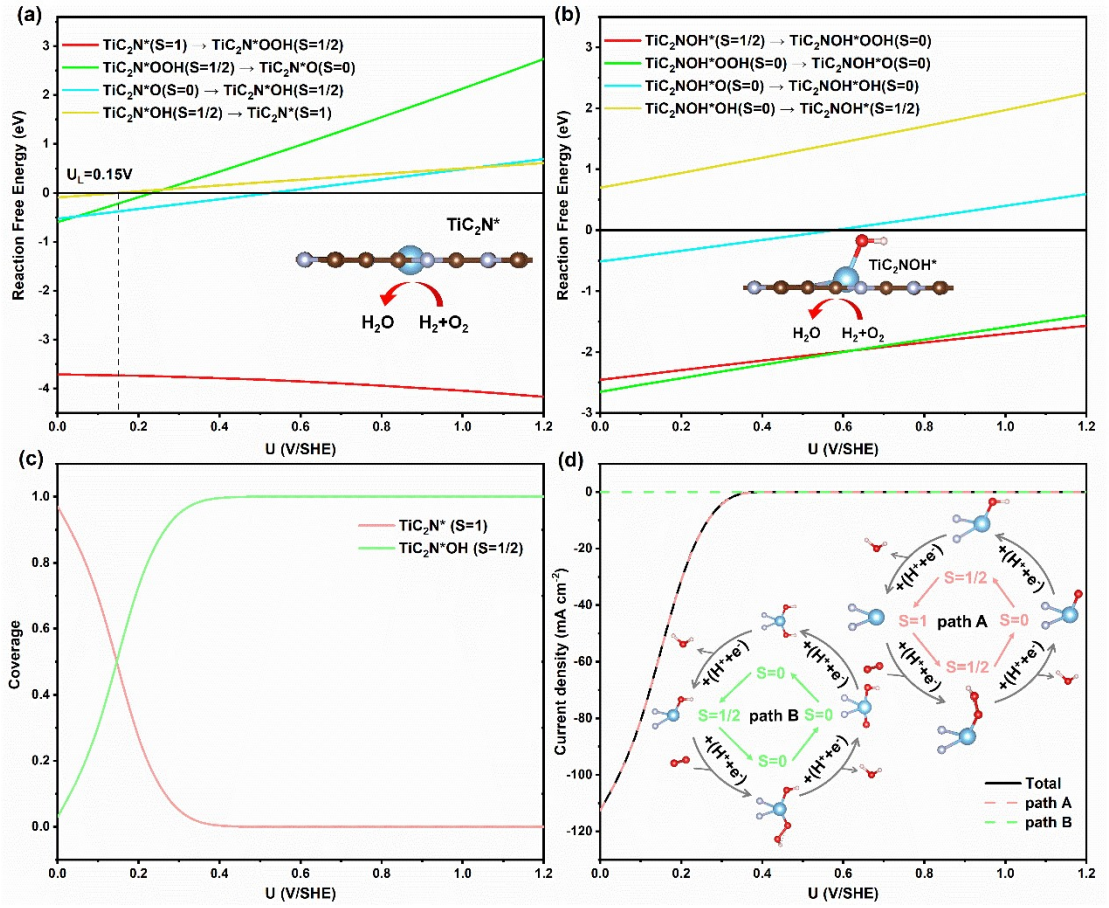

Figure S2. Constant-potential free energy of the ORR on (a) TiC_2N and (b) TiC_2N*OH; the coverage of TiC_2N and TiC_2N*OH vs. electrode potential; (d) simulation of total polarization current.

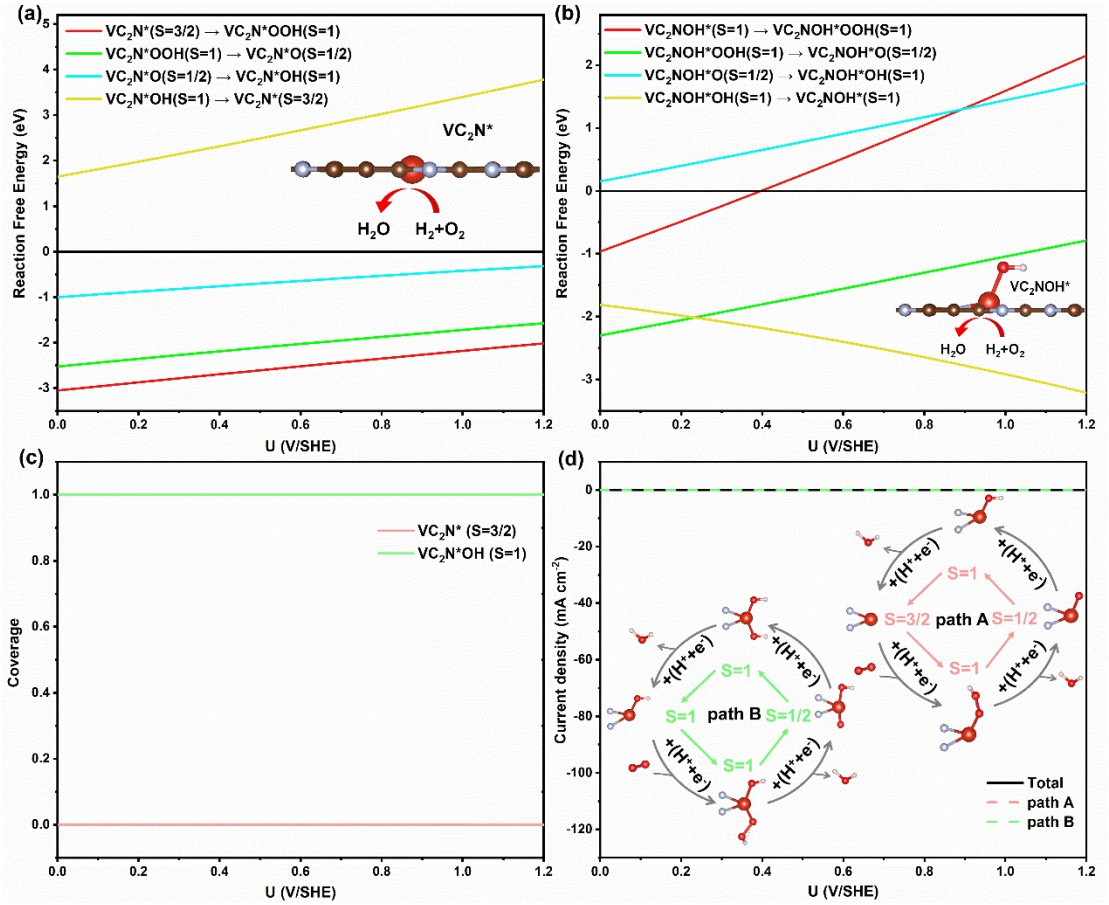

Figure S3. Constant-potential free energy of the ORR on (a) VC_2N and (b) VC_2N*OH; the coverage of VC_2N and VC_2N*OH vs. electrode potential; (d) simulation of total polarization current.

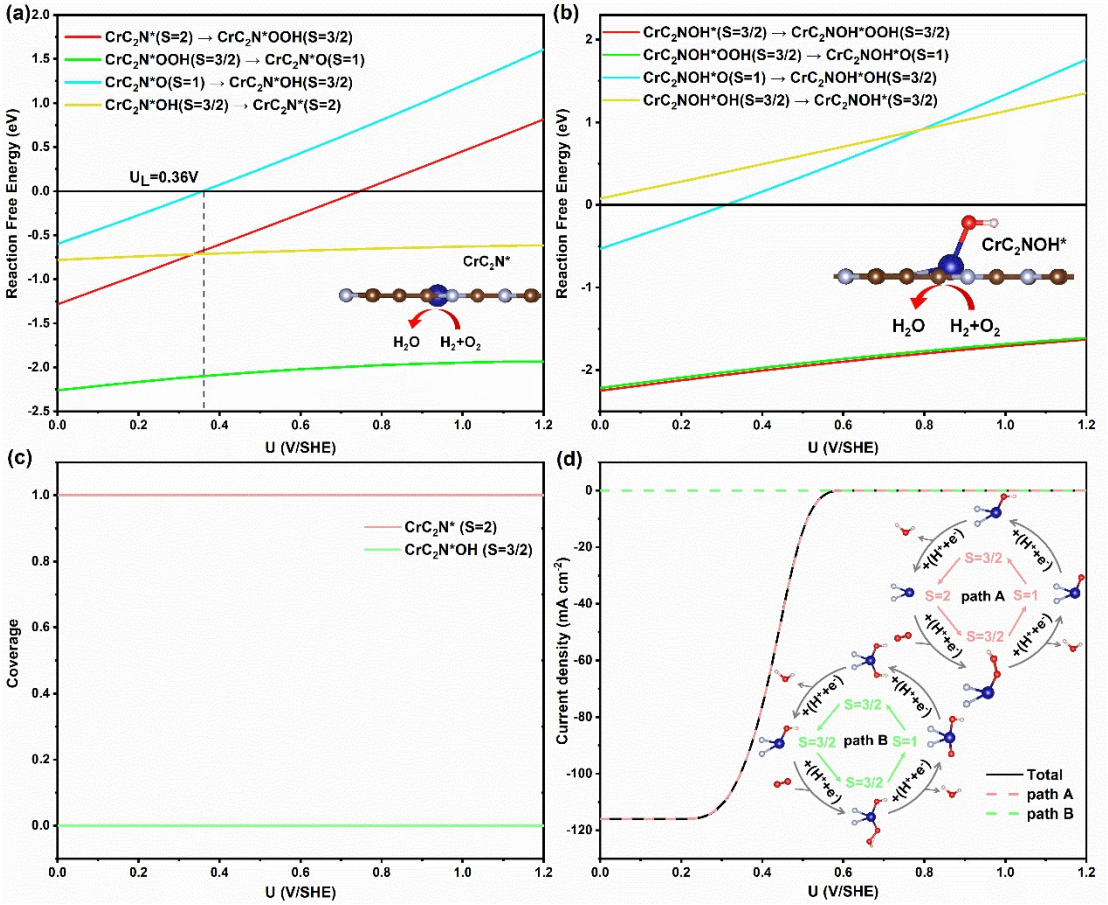

Figure S4. Constant-potential free energy of the ORR on (a) CrC_2N and (b) CrC_2N*OH; the coverage of CrC_2N and CrC_2N*OH vs. electrode potential; (d) simulation of total polarization current.

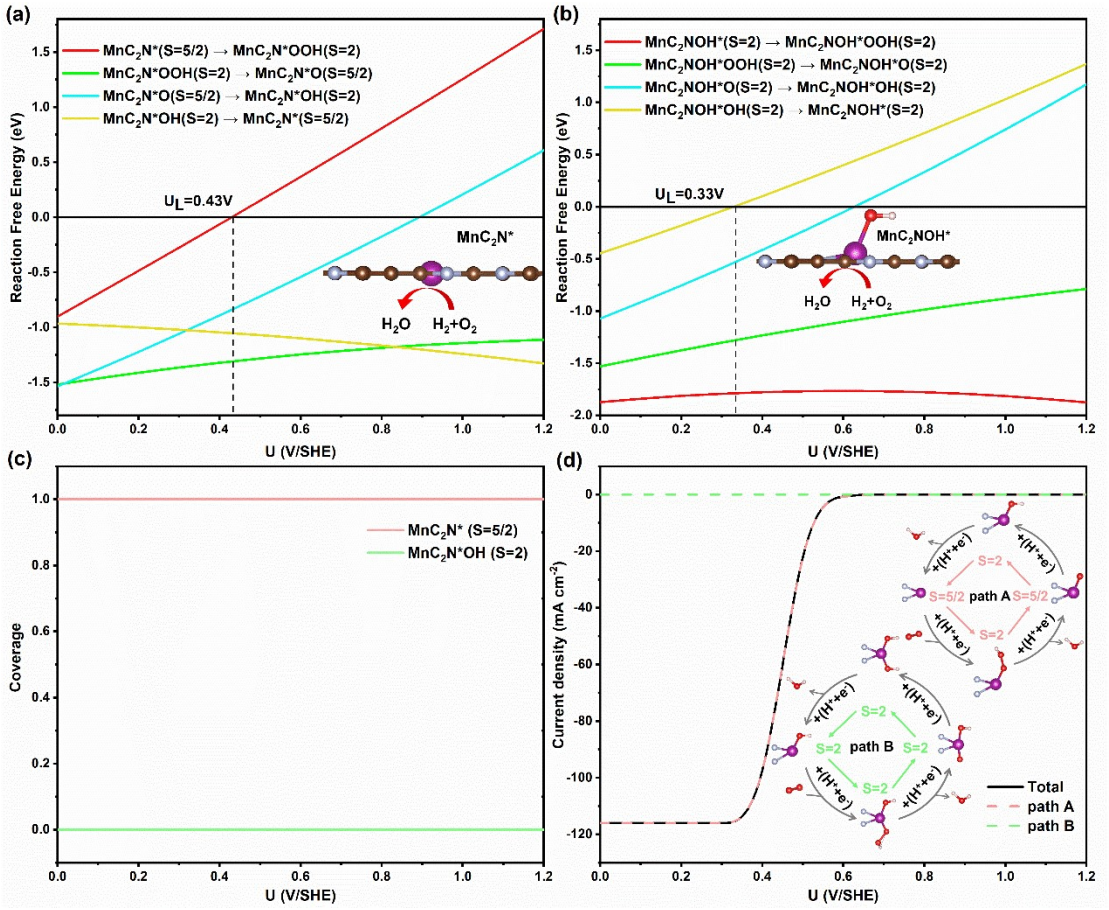

Figure S5. Constant-potential free energy of the ORR on (a) MnC_2N and (b) MnC_2N*OH; the coverage of MnC_2N and MnC_2N*OH vs. electrode potential; (d) simulation of total polarization current.

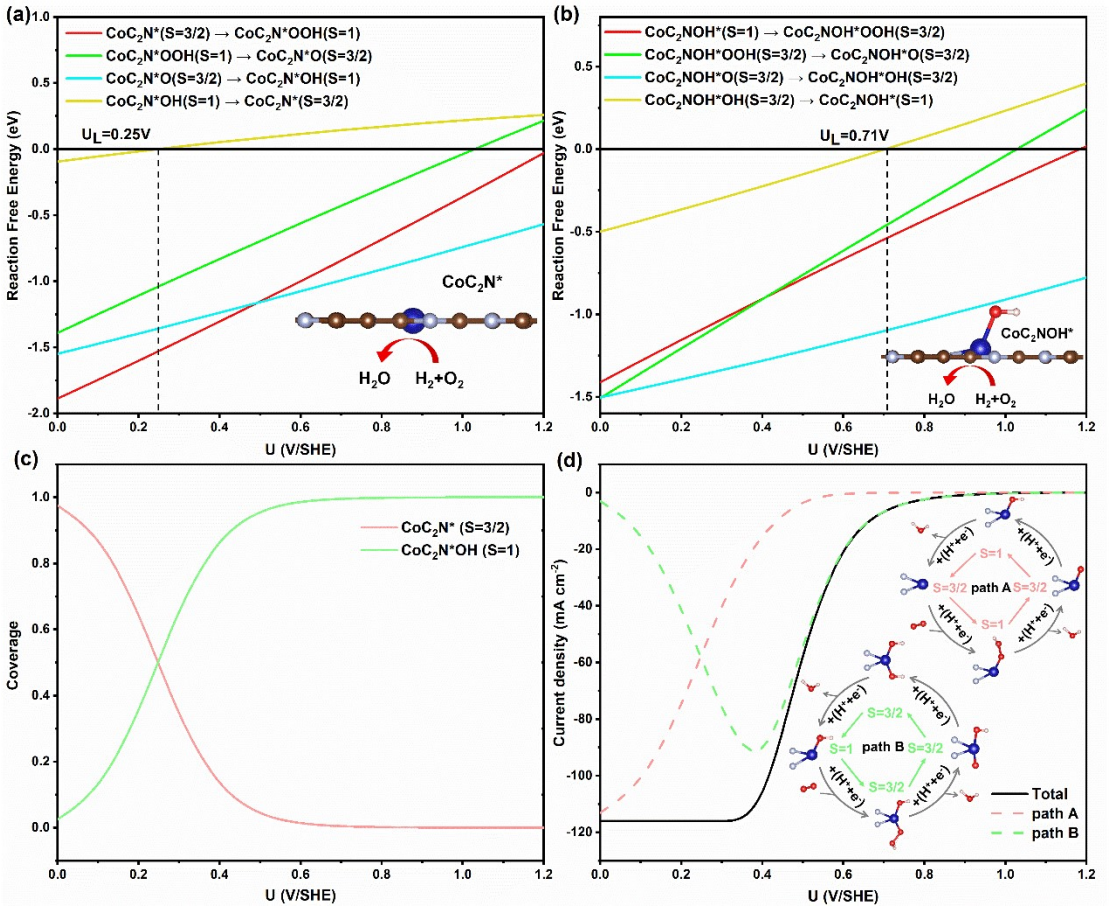

Figure S6. Constant-potential free energy of the ORR on (a) CoC_2N and (b) CoC_2N*OH; the coverage of CoC_2N and CoC_2N*OH vs. electrode potential; (d) simulation of total polarization current.

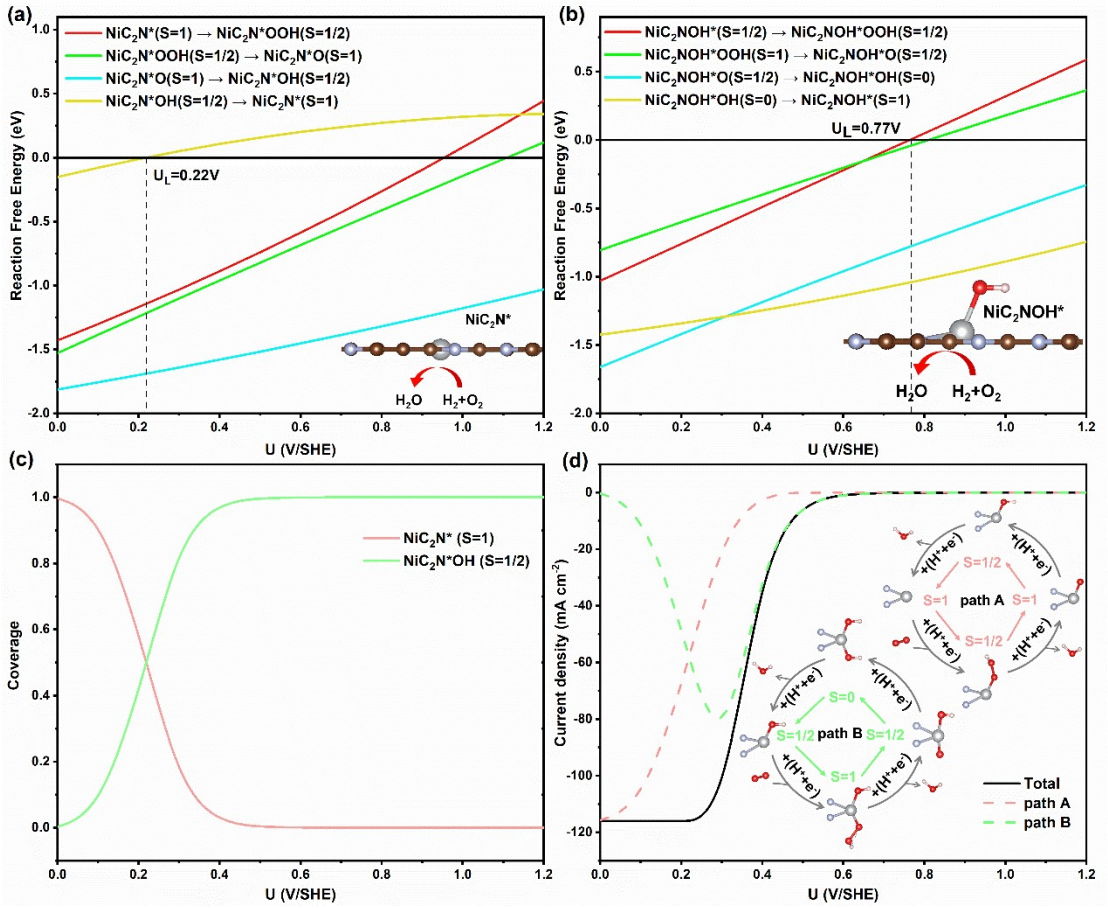

Figure S7. Constant-potential free energy of the ORR on (a) NiC_2N and (b) NiC_2N*OH; the coverage of NiC_2N and NiC_2N*OH vs. electrode potential; (d) simulation of total polarization current.

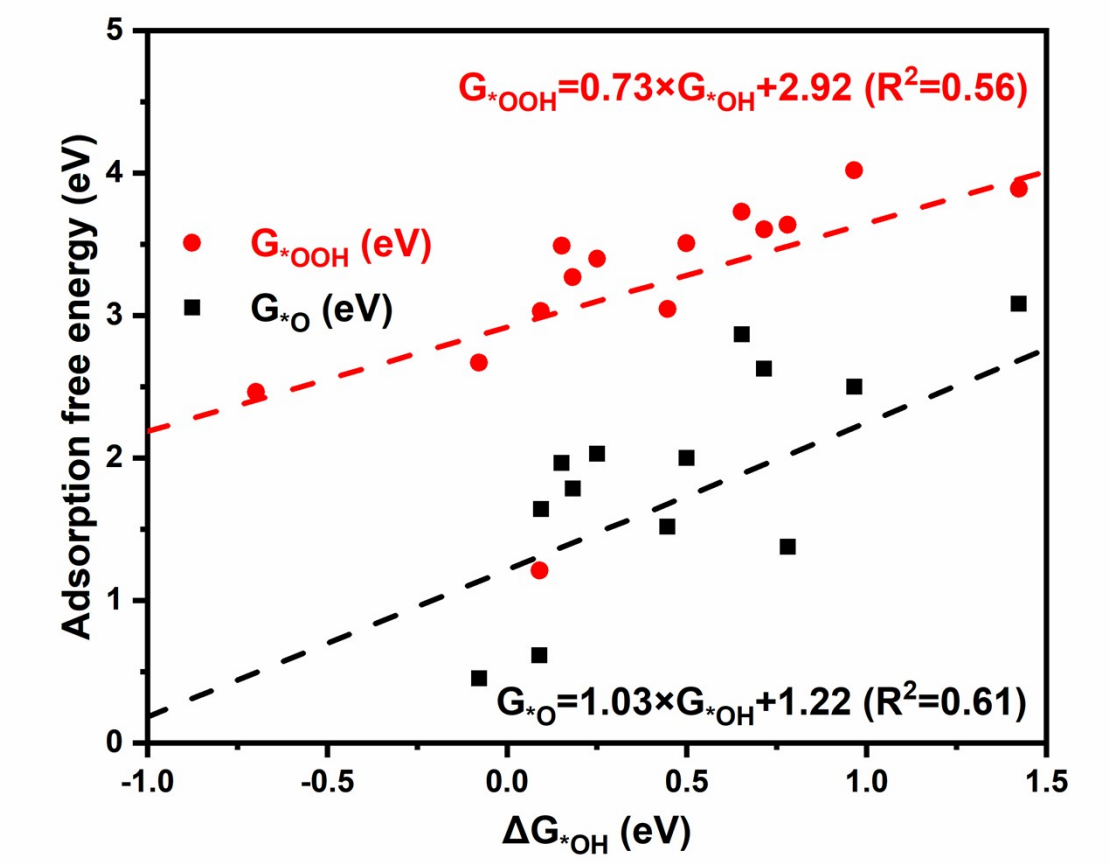

Figure S8. The linear fitting of adsorption free energy of G_{*OOH} and G_{*O} vs. G_{*OH}

References:

1. Y. Wang, Y.-J. Tang and K. Zhou, *J. Am. Chem. Soc.*, 2019, **141**, 14115-14119.
2. D. T. Limmer, A. P. Willard, P. Madden and D. Chandler, *Proc. Natl. Acad. Sci.*, 2013, **110**, 4200-4205.
3. Z. Huang and Q. Tang, *J. Phys. Chem. C* . 2022, **126**, 21606-21615.
4. H. A. Hansen, V. Viswanathan and J. K. Nørskov, *J. Phys. Chem. C* . 2014, **118**, 6706-6718.